ACES Asian Chemical Editorial Society

DOI: 10.1002/asia.201901771

CHEMISTRY AN ASIAN JOURNAL Full Paper

Special Collection

Asymmetric Hydroformylation Using a Rhodium Catalyst Encapsulated in a Chiral Capsule

Lukas J. Jongkind and Joost N. H. Reek*[a]

Abstract: Supramolecular capsules can be used to change the activity and selectivity of a catalyst through the influence of the second coordination sphere, reminiscent of how enzymes control the selectivity of their processes. In enzymes, this approach is used to also control the enantioselectivity of reactions in which the active catalytic site is often not chiral but the second coordination sphere is. We are interested in the possibility to generate a chiral second coordination sphere around an otherwise achiral transition metal complex for asymmetric catalysis. In this paper we show that the ligand template approach can be used to generate a chiral second coordination sphere around a rhodium complex, which is used in asymmetric hydroformylation.

One of the most important challenges in catalysis is to control the outcome of chemical reactions to produce key molecules in an efficient and selective manner. In homogeneous catalysis researchers mainly use ligands to control the activity and selectivity of transition metal complexes that are applied as catalysts in reactions.[1] The development of different ligand structures and the increased understanding of the chemical reactions that occur during catalysis has allowed researchers to develop specific ligand structures required for selective processes for different transition metals. In recent years, the development of supramolecular strategies in homogeneous catalysis has gained popularity as a new way to control the activity and selectivity of transition metal complexes.[2–8] Some supramolecular strategies aim to control the selectivity and activity of a catalytic reaction through the second coordination sphere of transition metal catalysts, which resembles the way enzymes control catalytic reactions. These efforts resulted in systems that operate via enzyme-like mechanisms such as substrate preorganization, transition state stabilization and cofactor controlled regulation.[9–18] These effects can be achieved by the encapsulation of transition metal complexes in supramolecular cages and capsules.[5,19–24] For these types of systems the confinement effect that is induced by the encapsulation is important, as different product selectivity and rate enhancement may be induced as an effect of catalyst encapsulation.

In our group we have used functionalized ligands to facilitate the encapsulation of transition metal complexes in a strategy we coined the ligand template approach.[25] In this approach, the ligand bears a central donor atom, usually a phosphorus atom, for coordination to a transition metal atom. Orthogonal donor atoms, predominantly harder donors such as nitrogen, are present in the ligand that can coordinate to bulky molecular building blocks in order to encapsulate the central donor atom of the ligand and the transition metal center bound to it. Using this approach, we have encapsulated several transition metal complexes to demonstrate the effect of encapsulation in catalysis.

The first example of the ligand template approach involves the encapsulation of the tris-3-pyridyl phosphine ligand template with zinc tetraphenyl porphyrin (Zn(II)TPP).[26–29] The phosphine atom selectively coordinates to rhodium, while the pyridine donor atoms coordinate to the zinc atoms of the Zn(II)TPP, encapsulating the rhodium complex. When this capsule is applied in the rhodium catalyzed hydroformylation of unfunctionalized alkenes, the formation of aldehyde products on the innermost position of the alkene as the major product. As no traditional ligand system is known that shows a similar product selectivity, this capsule was studied in detail, which revealed that the unique product selectivity is caused by hindered rotation enforced by the capsule during hydride migration.[28] Encapsulation of the ligand template changes the sterics, which leads to the formation of a rhodium catalyst coordinated to a single phosphine ligand, which partially explains the tenfold increase in activity as compared to the non-encapsulated ligand template observed.[26] Transition state stabilization induced by the encapsulation of the catalyst also contributes to the rate acceleration observed upon encapsulation.[28,30]

The ligand template approach was also successfully applied in enantioselective hydroformylation reactions, where encapsulation of a chiral ligand template led to increased enantioselectivity for both styrene and 2-octene hydroformylation.[31–33] In these examples the ligand template is the source of chirality, with encapsulation increasing the enantioselectivity of the catalyst.

[a] Dr. L. J. Jongkind, Prof. Dr. J. N. H. Reek
Homogeneous, Supramolecular and Bio-Inspired Catalysis
Van't Hoff Institute for Molecular Sciences
University of Amsterdam
Science Park 904, 1098 XH Amsterdam (The Netherlands)
E-mail: j.n.h.reek@uva.nl

Supporting information for this article is available on the WWW under https://doi.org/10.1002/asia.201901771

This manuscript is part of a special collection in honor of the 2nd International Conference on Organometallics and Catalysis (ICOC-2020). Click here to see the Table of Contents of the special collection.

Enzymes achieve perfect enantioselectivity solely through the chirality of second coordination sphere.[34] Inspired by this, we were interested whether the use of an achiral ligand template and chiral capsule building blocks could generate a chiral capsule for enantioselective hydroformylation. Because the application of the tris-3-pyridyl phosphine ligand template (ligand template **1**) encapsulated by Zn(II)TPP in rhodium catalyzed hydroformylation of unfunctionalized alkenes produces chiral aldehydes (as a racemic mixture) as major products, we chose the encapsulation of ligand template **1** with chiral porphyrins to form a chiral capsule for enantioselective hydroformylation (Figure 1). Here we discuss the synthesis of suitable porphyrin building blocks, the encapsulation of ligand template **1** with these porphyrins and the application of the formed capsules in rhodium catalyzed hydroformylation.

Results and discussion

Ligand template **1** has been studied thoroughly in previous research, providing guidelines for encapsulating this ligand template in a fashion that would allow for chiral induction in catalysis.[30,35,36] The ligand template in solution is highly dynamic, as the pyridine groups can rotate freely in solution. When the ligand template is encapsulated by porphyrins the number of possible conformations the ligand template can adopt is decreased due to steric restrictions imposed by the coordination of the porphyrins.[35,36] The capsule formed by encapsulation of ligand template **1** with Zn(II)TPP is present in only two different conformation in the crystal structure.[30] Inspection of these structures shows that for both structures the pyridine groups are pointing in the same direction, creating a propeller shape. The difference between the two propeller conformations is the handedness of the propeller, making these two observed conformations a pair of enantiomeric conformers (Figure 2). Interconversion between the two enantiomeric forms can only occur when one of the capsule building blocks is dissociated, whereafter the conformation can flip to the propeller conformation of opposite handedness. Porphyrin association and dissociation and therefore the interconversion between the two enantiomeric conformations is fast on the NMR timescale, also at low temperatures down to −90 °C, and as such both enantiomeric forms of ligand template **1** are present in solution.[35,36]

When ligand template **1** could be encapsulated by chiral porphyrin building blocks, the two resulting conformers of opposite handedness would be diastereoisomers that may have different energies. In that case, the ligand template adapts to form the lower energy conformer as the major product, essentially creating a *diastereomeric excess* of that conformation, resulting in a capsule that can be applied in enantioselective catalysis.

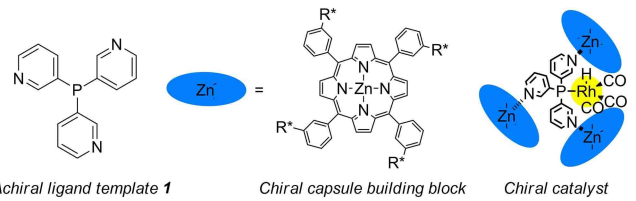

Figure 1. Achiral ligand template **1** encapsulated with chiral capsule building blocks, explored as asymmetric catalysts in hydroformylation in this work.

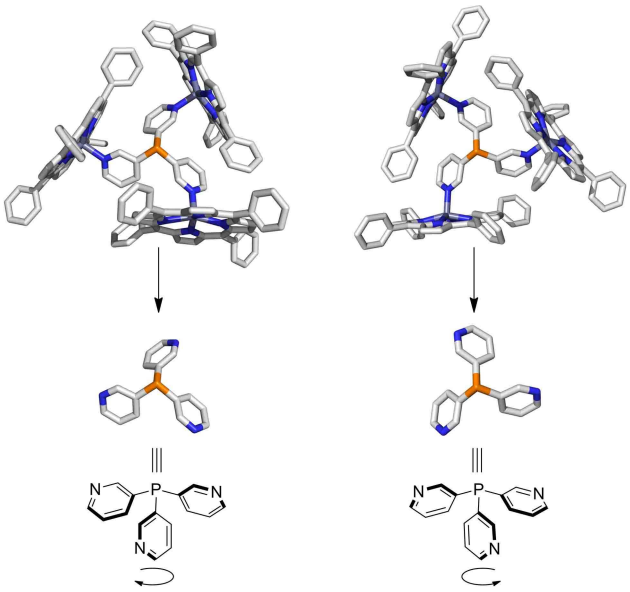

Figure 2. Encapsulation of ligand template **1** with Zn(II)TPP limits the amount of possible conformations of the ligand template to two distinct conformations, as observed in the crystal structure (top), two enantiomeric propeller conformations of the ligand template (middle and bottom).

Synthesis

From previous research it is known that the shape of the capsule is essential for achieving highly branched selectivity in hydroformylation. The shape suitable for selective hydroformylation catalysis is only preserved for capsules based on substituted porphyrins with the substituent at the *meta* position of the phenyl rings of the tetraphenyl porphyrin.[28] The *meta* substituent is known not to disrupt the intermolecular CH-π interactions required for the formation of the capsule, as the substituents are pointing away from the center of the capsule.[30] When porphyrins with *ortho* or *para* substituents are used, steric hindrance causes deformation of the capsule.

We synthesized several chiral porphyrins to serve as capsule building blocks for the generation of encapsulated catalysts. These porphyrins were synthesized using two strategies. The synthesis of chiral porphyrin **2** was achieved through introduction of a chiral carboxamide onto a bromo-substituted porphyrin using similar Buchwald-Hartwig amination conditions as described in literature (see experimental section for details),[37] followed by methylation of the amide functionalities in order to obtain desirable solubility properties, and metalation (scheme 1). All intermediates in these reactions were characterized by NMR spectroscopy and high-resolution mass spec-

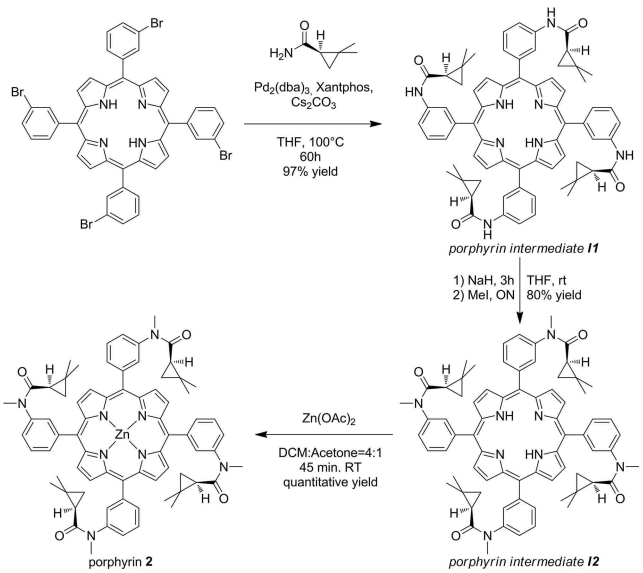

Scheme 1. Synthesis of chiral porphyrin **2** using Buchwald-Hartwig amination.

trometry (HR-MS, for the spectra see SI). Similar to porphyrins reported in literature, no diastereoisomers were observed in the ^{1}H NMR, indicating that no racemization of the chiral groups had occurred during the synthesis.[37]

Porphyrins **3**–**5** were synthesized by ester condensation of the hydroxyl substituted porphyrins with chiral acids and subsequently metalated to provide the chiral zinc porphyrins (scheme 2). For porphyrins **3**–**5**, the intermediate species (not depicted in scheme 2) and the final products were characterized by NMR spectroscopy and HR-MS (for spectra see SI). No diastereoisomers were observed according to ^{1}H NMR, indicating retention of the chiral configuration of the substituents throughout these reactions.

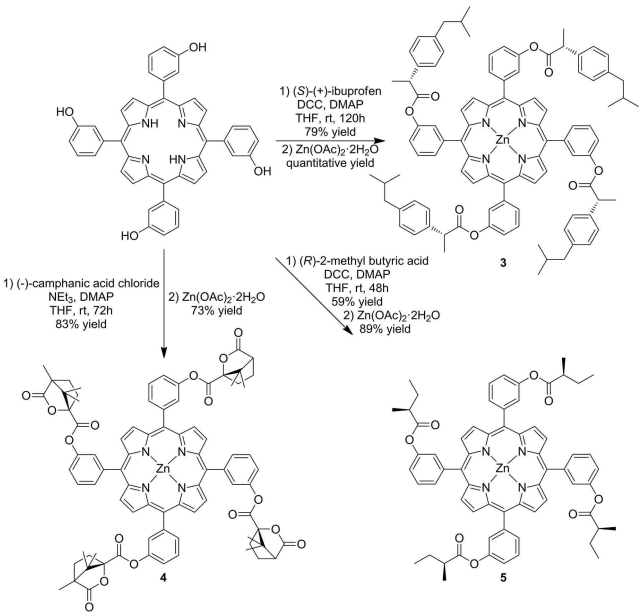

Scheme 2. Synthesis of porphyrin **3**–**5** through ester condensation.

Formation of encapsulated catalysts

DFT calculations of the capsule formed from ligand template **1** and porphyrin **2** indicate that the computed structures are similar to the structures known for the Zn(II)TPP capsule (Figure 3 and 4, Carthesian coordinates provided in the SI). The chiral substituents are pointing outwards, unable to have direct contact with a metal that is coordinated at the inside of the capsule. The source for any chiral induction in catalysis should therefore originate from the chirality of the conformation of ligand template **1** in combination with the chiral shape of the porphyrin capsule. The two calculated structures of the diasteomeric forms of the capsule have an energy difference of 3 kcal/mol, indicating that if the capsule forms in solution one of the diastereomeric forms will be the major conformer present. The calculated structures were compared with the structure of the ZnTPP based capsule (figure 4). The overlay of the structures shows that for the capsules based on porphyrin **2** (in red and yellow) two of the porphyrins are in a similar conformation as is observed for the ZnTPP capsule (in blue). The third porphyrin is rotated compared to the ZnTPP capsule and for the rotated porphyrins no CH-π between the porphyrin and the other porphyrin building blocks are observed. This suggests that for the capsule based on porphyrin **2** the binding of the last porphyrin building blocks may not exhibit the cooperative binding effect observed for the ZnTPP capsule.[28,30] The distortion of the capsule shape when using porphyrin **2** as

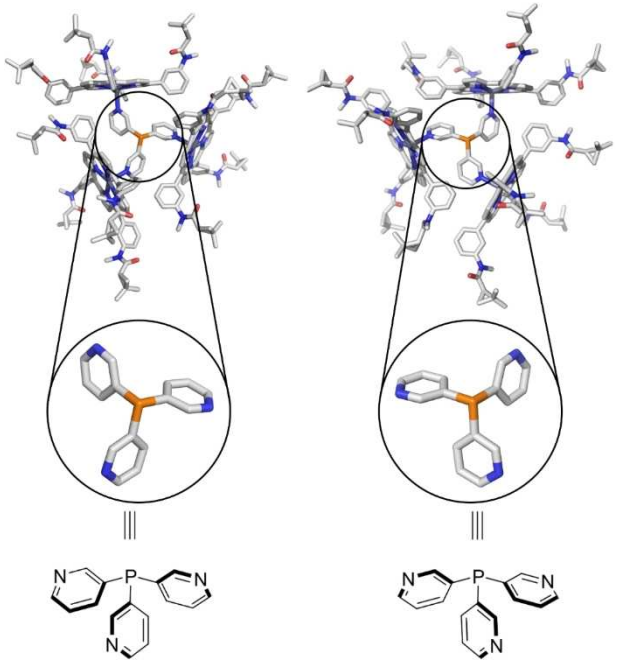

Figure 3. DFT calculations show that the energy difference between the two enantiomeric states of ligand template **1** is 3 kcal/mol when encapsulated with porphyrin **2**, lower energy structure depicted on the right.

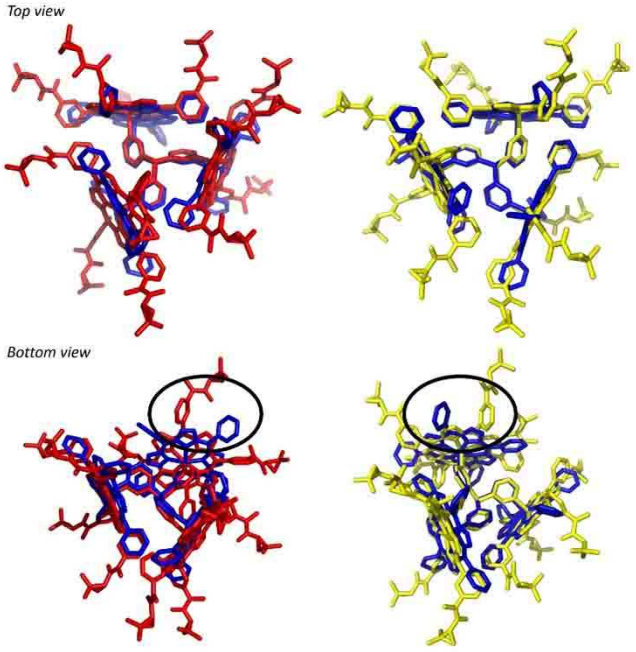

Figure 4. Overlay structure of the chiral enantiomeric states of the capsule formed by ligand **1** and porphyrin **2** with the capsule formed by encapsulation of ligand **1** with ZnTPP, viewed from the top (upper pictures) and from the bottom, showing that one of the porphyrins in the capsule formed with porphyrin **2** is rotated compared to the ZnTPP based capsule (lower pictures).

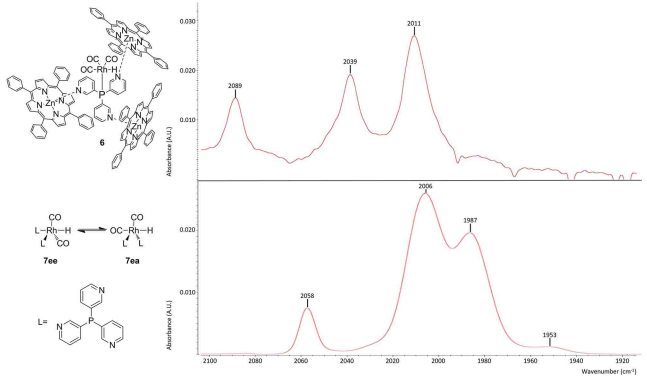

Figure 5. Active catalyst **6** is formed upon encapsulation of ligand template **1** with Zn(II)TPP in presence of a rhodium precursor under catalytic conditions, the HP-IR spectrum shows three characteristic carbonyl peaks at 2089, 2039 and 2011 cm^{-1} (top, [Rh] = 1.0 mM, [phosphine **1**] = 2.5 mM, [ZnTPP] = 7.5 mM). Catalyst **7** is formed by ligand template **1** and a rhodium precursor under catalytic conditions in absence of capsule building blocks, with the *equatorial-apical* (**ea**) and the *equatorial-equatorial* (**ee**) isomers leading to four peaks in the HP-IR at 2058, 2006, 1987 and 1953 cm^{-1} (bottom, taken from ref. [29]).

a capsule building block is a result of the chiral substituents on the porphyrin building block, which are in close proximity in several locations in the calculated structure. The influence of close proximity between the chiral substituents on the distorted binding of the third equivalent of porphyrin **2** to ligand template **1** explains why one of the diastereomeric conformations is lower in energy.

To investigate if a capsule is formed around the rhodium atom when porphyrins **2**–**5** are used as capsule building blocks, we used high-pressure infrared (HP-IR) spectroscopy.[27,29,38] HP-IR can be used to observe IR stretch vibrations of the carbonyl ligands present around the rhodium center, which provides information about the geometry of the coordination complex. The electron density of the rhodium is influenced by the other ligands present in the complex, and this in turn influences the positions of the carbonyl IR bands. In the absence of porphyrin building blocks, a RhH(ligand **1**)$_2$(CO)$_2$ complex forms under syngas pressure, which will convert to a monocoordinated complex when the ligand template is successfully encapsulated by the porphyrin building blocks. The species formed under syngas pressure for ligand template **1** and various equivalents of Zn(II)TPP are well-known.[27–29] For the encapsulated catalyst, leading to a RhH(ligand **1**)(CO)$_3$ complex, three carbonyl frequencies are observed. For the non-encapsulated complex (RhH(ligand **1**)$_2$(CO)$_2$), two sets of two peaks are observed as a result of the formation of the **ee** and **ea** coordination complexes (figure 5).[27–29] Previous research also showed that formation of a bis-(3-pyridyl)phenylphosphine ligand template encapsulated with two Zn(II)TPP capsule building blocks leads to the formation of a mono-coordinated rhodium catalyst with three carbonyl peaks observed. The spectrum for the RhH(**1**·(ZnTPP)$_2$)(CO)$_3$ has not been recorded, but the HP-IR spectrum in that case will likely deviate by several wavenumbers from the spectrum observed for catalyst **6**.

The HP-IR spectra recorded for porphyrins **2**–**5** are all nearly identical to the spectrum recorded for catalyst **6** (see figure 6). Three peaks are observed, characteristic for the formation of a mono-coordinated rhodium species with three carbonyl ligands.[27,28] The IR stretch frequencies of the carbonyl ligands are within one reciprocal centimeter the same as for catalyst **6**, indicating that the carbonyl ligands have identical electronic properties. Below 2000 cm^{-1} no peaks are observed, ruling out the formation of a bis-coordinated species similar to catalyst **7**. These spectra indicate that under catalytic conditions, the species formed by encapsulation of ligand template **1** with porphyrins **2**–**5** are nearly identical to catalyst **6**, a mono-phosphine-coordinated rhodium species with three carbonyl ligands, encapsulated by three chiral porphyrin capsule building blocks.

Catalysis

The selectivity of the encapsulated catalysts based on ligand template **1** in the hydroformylation of 1-octene is strongly influenced by capsule formation.[26–28,30] Previous research has shown that when the ligand template is encapsulated with only two Zn(II)TPP building blocks, the resulting ratio between the linear and the branched aldehyde product (the l/b ratio) is 1.1.[27] When three Zn(II)TPP molecules are bound to the ligand template, a full capsule is formed around the rhodium atom, which leads to a characteristic l/b ratio of 0.60 when applied in 1-octene hydroformylation. Similar l/b ratios have been observed when *meta* substituted tetraphenyl porphyrins were

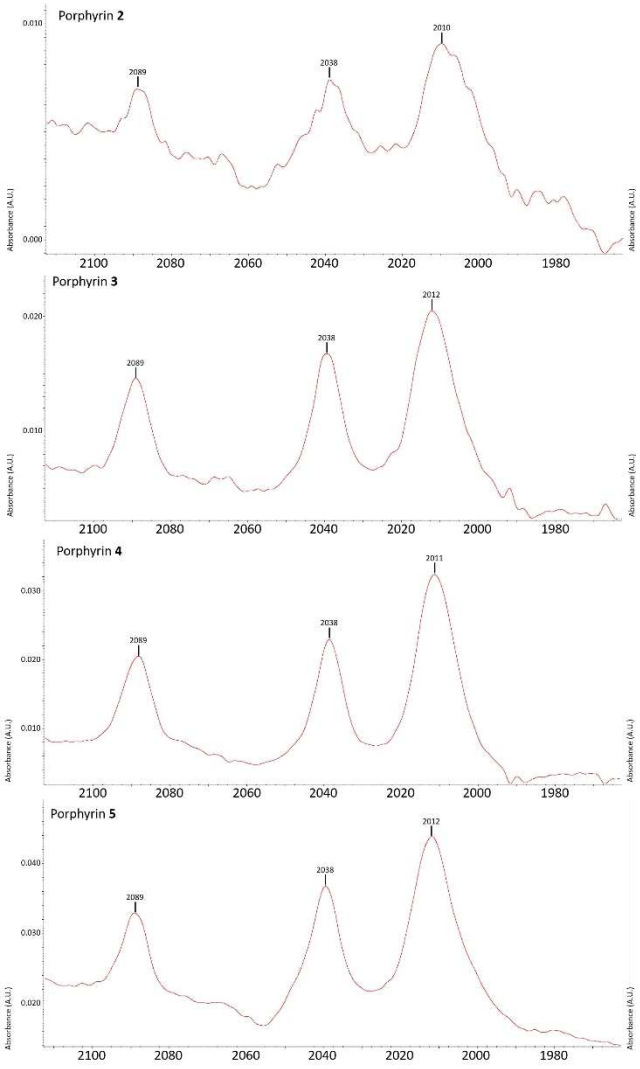

Figure 6. HP-IR spectra recorded for the active species formed by encapsulation of ligand template **1** in presence of a rhodium precursor and under syngas pressure ([Rh] = 1.0 mM, [phosphine **1**] = 2.5 mM, [Chiral porphyrin building blocks] = 7.5 mM in DCM) with porphyrin **2** (top left, carbonyl frequencies: 2089, 2038 and 2010 cm^{-1}), porphyrin **3** (top right, carbonyl frequencies: 2089, 2038 and 2012 cm^{-1}), porphyrin **4** (bottom left, carbonyl frequencies: 2089, 2038 and 2011 cm^{-1}) and porphyrin **5** (bottom right, carbonyl frequencies: 2089, 2038 and 2012 cm^{-1}).

used as capsule building blocks.[26,30] Because the difference in selectivity between the $RhH((1)(TPP)_3)(CO)_3$ and the $RhH((1)(TPP)_2)(CO)_3$ complexes in 1-octene hydroformylation is large, we first used our new capsules in this reaction to confirm proper capsule formation under catalytic conditions (table 1). The catalytic results show that when three equivalents of porphyrin **2** are present in the catalytic mixture, the l/b ratio of the product aldehydes is 0.90, suggesting that full encapsulation was not achieved. When porphyrin **2** is added in excess compared to ligand template **1** the l/b ratio of the product aldehydes is 0.56, which is the characteristic selectivity obtained for a capsule based on a three-to-one porphyrin to ligand template ratio. These results show that an excess of porphyrin can be used to ensure formation of a fully encapsulated catalyst

Table 1. Hydroformylation of 1-octene with porphyrins **2–5**.

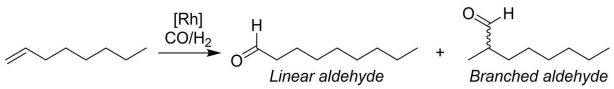

Porphyrin[a]	Substrate	Equivalents of porphyrin[b]	Yield [%][c]	l/b ratio[c]
2	1-octene	3	> 99	0.90
2	1-octene	6	> 99	0.56
3	1-octene	6	> 99	0.49
4	1-octene	6	> 99	0.50
5	1-octene	6	> 99	0.49

a] Conditions: $[Rh(acac)(CO)_2] = 0.18$ mM, [Rh]:[Phosphine **1**] = 1:5, [Rh]:[1-octene] = 1:400, T = 25 °C, t = 96 h, p = 20 bar ($CO:H_2 = 1:1$), solvent: Toluene. [b] with respect to ligand template **1**. [c] yield and l/b ratio determined with GC using decane as an internal standard, see experimental section for details.

when using porphyrin **2** as the capsule building block. The formation of three-to-one complexes of porphyrins **3–5** with ligand template **1** was also confirmed when an excess of porphyrin building blocks is present and the formed capsule are applied in 1-octene hydroformylation (table 1).

The 2-aldehyde was the major product formed during the hydroformylation of 1-octene, however we were unable to determine the enantioselectivity of the product formed (for attempts at separating the enantiomers see experimental section). Therefore the hydroformylation of 2-octene was attempted.[40] The capsule based on Zn(II)TPP has been shown to be an excellent catalyst for 2-octene hydroformylation, yielding up to 90% of the 3-aldehyde product.[28] Application of porphyrins **2–5** as capsule building blocks in the hydroformylation of 2-octene yielded no products, even when the catalyst loading (up to 1 mol%) and the temperature were increased (up to 40 °C). These results are in line with the previously reported results in which a *tetra*-3-nitrophenyl porphyrin was used to form the encapsulated catalyst which was applied in 2-octene hydroformylation, resulting in no conversion of the 2-octene. In that case the electron-withdrawing effect of the nitro substituent leads to the formation of a more stable capsule that blocked the conversion pathway for 2-octene and other internal alkenes.[28,30] For the capsules based on porphyrins **2–5** a combination of increased steric interaction caused by the substituents present and the electron-withdrawing nature of the substituents is likely to have the same effect.

Because no conversion was obtained for 2-octene hydroformylation, the capsule based on chiral porphyrin **2** was applied in styrene hydroformylation. The amount of porphyrin equivalents needed for the formation of a three-to-one capsule around ligand template **1** with porphyrin **2** was also investigated for this substrate. Application of three equivalents of porphyrin **2** in styrene hydroformylation showed that chiral induction is possible, yielding the product in 9% *enantiomeric excess* (*ee*) (Table 2). Adding porphyrin **2** in excess yielded a maximum *ee* of 13% when six equivalents of porphyrin are present. Addition of a larger excess of porphyrin **2** did not further increase the *ee*.

Table 2. Styrene hydroformylation with porphyrin **2** at different concentration.

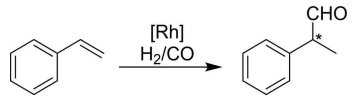

Porphyrin[a]	Substrate	Equivalents of porphyrin[b]	ee [%][c]
2	Styrene	3	9
2	Styrene	6	13
2	Styrene	9	13
2	Styrene	12	13

[a] Conditions: $[Rh(acac)(CO)_2]=0.18$ mM, [Rh]:[Phosphine **1**] = 1:5, T = 25 °C, t = 96 h, p = 20 bar ($CO:H_2=1:1$), solvent: Toluene. [b] with respect to ligand template **1**. [c] ee determined with chiral GC, see experimental section for details.

After having established the required conditions for successful capsule formation with the chiral porphyrins, the capsules based on porphyrins **2–5** were applied in the hydroformylation of several benchmark substrates (table 3, for further control experiments and examples of GC traces see SI). The encapsulated catalyst formed with porphyrin **2** shows the highest *ee* of all reactions performed, with 33% *ee* observed for the aldehyde product of vinyl acetate hydroformylation. Vinyl benzoate and vinyl pivalate hydroformylation products are formed with 16% and 15% *ee* respectively, at similar yield as for vinyl acetate. The product of styrene hydroformylation was formed in 13% *ee* with 92% yield. The capsule based on porphyrin **3** produces the aldehyde products of vinyl acetate, vinyl benzoate and vinyl pivalate in similar yields, around 70% and with an *ee* of around 20%. Compared to the capsule based on porphyrin **2**, the encapsulated catalyst formed with porphyrin **3** has a higher product yield, with lower *ee* observed for the products of vinyl acetate and styrene hydroformylation, but a higher *ee* for the products of vinyl benzoate and vinyl pivalate hydroformylation. The encapsulated catalyst formed with porphyrin **4** shows very low product yields with low *ee* of the product aldehydes. The capsule based on porphyrin **5** produces good yields, comparable to the capsules based on porphyrins **2** and **3**, but no significant amount of *ee* is observed in any of the product aldehydes.

Table 3. Asymmetric hydroformylation of several substrates with chiral porphyrin based capsules.

Porphyrin[a]	Substrate	Yield [%][b]	*ee*[c]
2	Vinyl acetate	45	33%
2	Styrene	96	13%
2	Vinyl benzoate	52	16%
2	Vinyl pivalate	45	15%
3	Vinyl acetate	71	19%
3	Styrene	99	6%
3	Vinyl benzoate	63	21%
3	Vinyl pivalate	76	18%
4	Vinyl acetate	11	12%
4	Styrene	13	3%
4	Vinyl benzoate	< 1	6%
4	Vinyl pivalate	< 1	4%
5	Vinyl acetate	56	2%
5	Styrene	98	< 1%
5	Vinyl benzoate	58	< 1%
5	Vinyl pivalate	69	< 1%

[a] Conditions: $[Rh(acac)(CO)_2]=0.18$ mM, [Rh] : [Phosphine **1**] = 1:5, [Phosphine **1**] : [Porphyrin] = 1:6, [Rh]:[substrate] = 1:1600, T = 25 °C, t = 96 h, p = 20 bar ($CO:H_2=1:1$), solvent, : Toluene. [b] determined with ^{1}H NMR using 1,3,5-trimethoxybenzene as an internal standard. [c] ee determined with chiral GC, see experimental section for details.

The results show that the influence of the chiral group attached to the porphyrin building block of the encapsulated catalyst is very important for the activity and selectivity of the reaction. The capsule based on porphyrin **2** has the highest *ee* aldehyde product for vinyl acetate, which is not increased by using a more sterically demanding substrate such as vinyl benzoate or vinyl pivalate. For the encapsulated catalyst formed with porphyrin **3** the *ee* and yield observed for all vinyl esters is similar, showing that for the encapsulated catalyst increasing the size of the substrate does not increase the selectivity of the reaction or inhibit the activity of the catalyst, as is observed for the catalyst formed with porphyrin **2**. The activity of the encapsulated catalyst is inhibited by the substituents on the capsule building blocks, as is observed for the capsule formed with porphyrin **4**. Similar to porphyrin **3**, the chiral groups of porphyrin **4** are connected to the porphyrin via ester bonds. The capsule based on porphyrin **4** yields low amounts of products for each substrate used, although the HP-IR of the encapsulated catalyst shows formation of the active rhodium hydride species. The low yield observed for the capsule based on porphyrin **4** is likely caused by the formation of a capsule that is too stable to accommodate catalysis, a results of the electronic and steric properties of the camphanic acid substituent on the capsule building blocks which is not a flexible or dynamic substituent. Porphyrin **5**, like porphyrins **3** and **4**, contains an ester bond to attach the chiral substituent to the porphyrin core. When porphyrin **5** is used for the formation of an encapsulated catalyst, no *ee* is detected in the product aldehydes. This is a result of the small size of the chiral substituents on porphyrin **5**, which are unable to steer the capsule formation process towards a chiral capsule.

Conclusion

We have shown that it is possible to perform enantioselective hydroformylation by encapsulating an achiral ligand template with chiral capsule building blocks. For this purpose several chiral porphyrins have been synthesized and characterized. Computational studies show that encapsulation of ligand template **1** limits the amount of conformations to two distinct conformations, which are diastereoisomers of one another that have different energies. The energy difference between the two diastereomeric conformations is 3 kcal/mol, which suggests that the capsule is almost exclusively present in that conformation. HP-IR spectra show that mono-coordinated catalysts are formed by ligand template **1** with chiral porphyrins **2–5** in presence of rhodium under syngas pressure. Titrations combined with catalysis data show that the chiral porphyrins have to be added in excess to form a three porphyrin to one ligand template

encapsulated state in catalysis. Application of the capsules based on porphyrins **2**–**5** in 1-octene hydroformylation yielded a linear to branched product ratio typical for these type of porphyrin based encapsulated catalysts. Application of the capsules based on porphyrins **2**–**5** in 2-octene hydroformylation gave no conversion of the substrate, which is caused by the formation of a more rigid capsule caused by the electronic properties and the increase steric interaction of the chiral substituents. When these catalysts are applied in asymmetric hydroformylation of various substrates, a maximum *ee* of 33% is achieved in the hydroformylation of vinyl acetate for the capsule formed by encapsulation with porphyrin **2**. The capsules based on porphyrin **2** and porphyrin **3** were found to produce the product aldehydes of all substrates with some amount of *enantiomeric excess*. Porphyrin **4** gave low conversion for all substrates owing to the formation of a cavity around the rhodium atom that cannot facilitate catalysis, similar to what was observed for all chiral porphyrins in 2-octene hydroformylation. Porphyrin **5**, which bears small chiral substituents, gave no *ee* for any of the substrates used, showing that the steric definition and size of the chiral substituents play an important role in enantioselective hydroformylation with these catalysts.

Experimental section

General procedures. All reactions were performed under an inert atmosphere (N_2 or Ar) using standard Schlenk techniques unless stated otherwise. Toluene was distilled over sodium under N_2 atmosphere before use. Styrene, vinyl acetate, vinyl benzoate and vinyl pivalate were filtered over basic alumina prior to use, 1,3,5-trimethoxybenzene and $Rh(acac)(CO)_2$ was used as received. Tris-3-pyridyl phosphine **1** was synthesized using literature procedures.[41]

HP-FTIR. High-pressure IR spectra were recorded using a specially modified autoclave.[42] The autoclave was flushed with Ar for 20 minutes prior to use. The samples were then injected under Ar flow, after which the autoclave was flushed with syngas (CO/H_2 = 1:1, 10 bar, 3x) and pressurized to the required pressure. Addition of Rh proceeded through a separate container in the autoclave under slight overpressure of syngas (25 bar). A background was measured of the phosphine ligand, the zinc porphyrin, after which $Rh(acac)(CO)_2$ was added and formation of the active species was monitored overnight. Concentrations used: [Rh] = 1.0 mM, [ligand template **1**] = 2.5 mM, [porphyrin] = 7.5 mM

Catalysis. Catalysis was performed in a stainless steel autoclave equipped with an eight vial insert, in which small GC vial (1.5 ml) were place loaded with a stirring bar. Porphyrins were weighed on a microbalance and added to the vials as solids. $Rh(acac)(CO)_2$ and 1,3,5-trimethoxybenzene were added as a stock solution in dry toluene and tris-3-pyridylphosphine was added as a stock solution in dry toluene prepared under inert conditions. All constituents were added to the vials after which the volume was completed to the required volume with dry toluene (typically 0.7 ml). These solutions were then stirred for 20 minutes under aerobic conditions, after which the vials were placed in the autoclave and the autoclave was flushed with syngas ($CO:H_2$ = 1:1, 3×20 bar) and pressurized to the required pressure. The autoclave was then placed in an oil bath set at the required temperature and stirred (750 rpm). After the required time, the reaction was halted by venting the syngas from the autoclave, after which the vials were removed and the solutions were used for analysis with ^{1}H NMR (take ~0.1 ml of solution and add 0.5 ml of $CDCl_3$) and chiral GC (Supelco β-dex 225 capillary column). Methods: Vinyl Acetate: 100 °C, hold for 10 min. then 4 °C/min to 140 °C; Styrene: 100 °C, hold for 5 min., then 4 °C/min to 160 °C, hold for 2 min.; Vinyl Benzoate: 135 °C, hold for 60 min.; Vinyl Pivalate: 77 °C, hold for 22 min. GC separation of the 1-octene hydroformylation products was performed on an Interscience Trace GC Ultra machine with a RTX-1 column (30 meter column, 0.25 mm internal diameter, 0.25 μm film thickness), initial temperature: 50 °C, hold for 2 minutes, ramp 10 °C/min to 300 °C, hold for 3 minutes.

Separation of 2-methyl octanal enantiomers. To separate the branched product isomer of the 1-octene hydroformylation several methods were attempted. Separation of the enantiomers with the Supelco β-dex 225 capillary column gave no separation of the products. Attempts at reduction of the aldehyde with $NaBH_4$ followed by either GC or HPLC were unreliable. Condensation of the product aldehydes with a chiral amine resulted in the formation of highly complex ^{1}H NMR spectra, for which we were unable to determine which peaks belonged to which products.

DFT calculations. Geometry optimizations were performed with the Amsterdam Density Functional (ADF) program using the BLYP functional and the DZP basis set similar to with previous calculations performed on these type of capsules.[30] The structures were generated using the two conformations observed in the X-ray structure of **1**$(Zn(II)TPP)_3$.

Synthesis

Porphyrin intermediate **i1**. Under N_2 atmosphere, 5,10,15,20-tetrakis (3-bromophenyl)porphyrin (99.0 mg, 0.1 mmol), (S)-(+)-2,2-Dimethylcyclopropanecarboxamide (364.2 mg, 3.2 mmol), Pd_2dba_3 (34.8 mg, 0.033 mmol), Xantphos (49.1 mg, 0.08 mmol) and Cs_2CO_3 (517.4 mg, 1.6 mmol) were added to a flame-dried Schlenk flask, followed by the addition of dried THF (6 ml) after which the mixture was stirred for 60 h at 100 °C. After the reaction was cooled down to RT, DCM (50 ml) was added and solids were removed through filtration. The solvent was then removed and the product was purified using column chromatography (SiO_2, DCM:Acetone = 20:1) yielding the product as a purple solid (109.0 mg, 0.1 mmol) in 97% yield. ^{1}H NMR (300 MHz, Acetone-d_6) δ 9.73 (s, 4H), 8.97 (s, 8H), 8.58 (d, J = 8.3 Hz, 4H), 8.21 (d, J = 8.1 Hz, 4H), 7.94 (d, J = 7.6 Hz, 4H), 7.73 (t, J = 7.9 Hz, 4H), 1.75 (t, J = 6.7 Hz, 4H), 1.23 (s, 12H), 1.16 (s, 12H), 1.11 (d, J = 5.0 Hz, 4H), 0.80 (dd, J = 8.0, 3.9 Hz, 4H), −2.74 (s, 2H). ^{13}C NMR (75 MHz, Acetone-d_6) δ 169.8, 142.5, 138.3, 129.3, 128.9, 128.2, 127.3, 127.1, 125.3, 120.1, 118.2, 26.5, 22.0, 19.8, 18.1. HR-MS (CSI+): calculated for $[MH]^+$ ($C_{68}H_{66}N_8O_4$): 1059.5285, found: 1059.5330

Porphyrin intermediate **i2**. Under N_2 atmosphere, porphyrin intermediate **i1** (101.8 mg, 0.10 mmol) and NaH (60% dispersion in mineral oil, 40.7 mg, 1.7 mmol) were dissolved in dry THF (10 ml), after which the solution was stirred for 3 h at RT. Subsequently, MeI (120 μl, 1.9 mmol) was added and the mixture was stirred overnight. After evaporating the solvent, the product was purified using column chromatography (SiO_2, DCM:Acetone = 3:1) yielding the product as a purple solid (87.1 mg, 0.08 mmol) in 81% yield. ^{1}H NMR (300 MHz, Chloroform-*d*) δ 9.06–8.67 (m, 8H), 8.32–8.02 (m, 8H), 7.85 (td, J = 7.8, 3.2 Hz, 4H), 7.68 (d, J = 8.0 Hz, 4H), 3.60 (s, 12H), 1.36–1.25 (m, 8H), 1.13 (s, 12H), 0.94 (s, 12H), 0.74 (dd, J = 7.9, 4.2 Hz, 4H), −2.77 (s, 2H). ^{13}C NMR (75 MHz, Chloroform-*d*) δ 171.5, 143.3, 143.0, 133.1, 130.9, 128.8, 127.7, 119.2, 37.7, 29.7, 28.8, 26.5, 22.3, 20.4, 19.0, 18.1. HR-MS (CSI+): calculated for $[MH]^+$ ($C_{72}H_{74}N_8O_4$): 1115.5911, found: 1115,5932

Chiral porphyrin **2**. Porphyrin intermediate **i2** (87.1 mg, 0.07 mmol) and $Zn(OAc)_2$ (179.9 mg, 0.98 mmol) were dissolve in a mixture of DCM (25 ml) and Acetone (10 ml) and stirred for 1 h at RT, after which the solvent was evaporated. The residue was then dissolved in EtOAc (50 ml) and washed with water (3×50 ml), after which the organic layer was dried with Na_2SO_4, filtered and evaporation yielded the product as a purple solid (90.4 mmol, 0.07 mmol) in quantitive yield. ^{1}H NMR (300 MHz, Chloroform-*d*) δ 8.88 (br m, 8H), 8.27–8.06 (m, 4H), 7.96 (d, *J* = 12.4 Hz, 4H), 7.78 (q, *J* = 6.2, 5.2 Hz, 4H), 7.55 (s, 4H), 3.32 (br s, 12H), 1.33–1.20 (m, 4H), 0.94 (br m, 14H), 0.60 (s, 5H). ^{13}C NMR (75 MHz, Methylene Chloride-d_2) δ 170.5, 149.9, 149.8, 144.5, 142.2, 132.8, 132.6, 131.7, 131.5, 127.2, 126.3, 119.5, 29.7, 28.0, 25.9, 21.6, 18.3. HR-MS (CSI+): calculated for $[MH]^+$ ($C_{72}H_{72}N_8O_4Zn$): 1178.4968, found 1178.5046

Porphyrin **i3**. Under N_2 atmosphere, 5,10,15,20-tetrakis(3-hydroxyphenyl)porphyrin (294.3 mg, 0.43 mmol), (S)-(+)-Ibuprofen (481.9 mg, 2.4 mmol), DCC (532.4 mg, 2.6 mmol) and DMAP (29.2 mg, 0.24 mmol) were dissolved in dry THF (15 ml) and stirred for 120 h at RT. After this, the solvent was evaporated and the product was isolated using column chromatography (SiO_2, DCM: Hexane = 10:1) yielding the product as a purple solid (505 mg) in 79% yield. ^{1}H NMR (300 MHz, Methylene Chloride-d_2) δ 8.93 (s, 8H), 8.10 (d, *J* = 7.7 Hz, 4H), 7.92 (s, 4H), 7.79 (t, *J* = 7.9 Hz, 4H), 7.50 (d, *J* = 8.0 Hz, 4H), 7.37 (d, *J* = 7.7 Hz, 8H), 7.15 (d, *J* = 7.7 Hz, 8H), 4.08 (q, *J* = 7.1 Hz, 4H), 2.44 (d, *J* = 7.2 Hz, 8H), 1.80 (hept, *J* = 7.0 Hz, 4H), 1.67 (dd, *J* = 7.1, 2.4 Hz, 12H), 0.85 (d, *J* = 6.6 Hz, 24H), −2.91 (s, 2H). ^{13}C NMR (75 MHz, Chloroform-*d*) δ 173.4, 149.5, 143.2, 140.8, 137.2, 132.1, 130.9, 129.6, 127.6, 127.5, 127.2, 120.9, 119.0, 45.4, 45.0, 30.1, 29.7, 22.4, 18.6, 14.1. HR-MS (CSI+): calculated for $[MH]^+$ ($C_{96}H_{94}N_4O_8$): 1432.7183, found 1432.7149

Zinc porphyrin **3**. Porphyrin **i3** (505.3 mg, 0.34 mmol) and $Zn(OAc)_2 \cdot 2H_2O$ (1.1 g, 5.0 mmol) were dissolved in a mixture of DCM (15 ml) and Acetone (10 ml) and stirred for 1.5 h at RT. After this, the solvent was evaporated, the residue was dissolved in EtOAc (50 ml) and washed with H_2O (3x 50 ml), dried with $MgSO_4$ and filtered. The product was obtained by evaporation of the solvent, yielding the product as a purple solid (520 mg) in quantative yield. ^{1}H NMR (300 MHz, Chloroform-*d*) δ 9.01 (s, 8H), 8.07 (d, *J* = 7.5 Hz, 4H), 7.91 (s, 4H), 7.73 (t, *J* = 7.9 Hz, 4H), 7.47 (d, *J* = 8.2 Hz, 4H), 7.41–7.32 (m, 8H), 7.19–7.03 (m, 8H), 4.05 (q, *J* = 7.6 Hz, 4H), 2.43 (d, *J* = 7.2 Hz, 8H), 1.94–1.75 (m, 4H), 1.68 (d, *J* = 3.7 Hz, 12H), 0.86 (d, *J* = 6.5 Hz, 24H). ^{13}C NMR (75 MHz, Chloroform-*d*) δ 173.4, 150.1, 149.4, 143.9, 140.8, 137.2, 132.2, 131.9, 129.5, 127.5, 127.3, 127.2, 120.7, 120.0, 45.4, 45.0, 30.1, 22.4, 18.6. HR-MS (CSI+): calculated for $[MH]^+$ ($C_{96}H_{92}N_4O_8Zn$): 1494.6224, found 1494.6271

Porphyrin **i4**. Under N_2 atmosphere, 5,10,15,20-tetrakis(3-hydroxyphenyl)porphyrin (200.0 mg, 0.29 mmol), (−)-camphanic acid chloride (286.6 mg, 1.3 mmol) and DMAP (13.2 mg, 0.12 mmol) were added to a Schlenk flask and dissolved in THF (10 ml), after which NEt_3 (0.2 ml, 1.5 mmol) was added and the mixture was stirred for 72 h at RT. After this, the solvent was removed and the mixture was purified using column chromatography (SiO_2, DCM: Hexane = 20:1), yielding the product after evaporation of the solvent as a purple solid (327.4 mg) in 83% yield. ^{1}H NMR (300 MHz, Chloroform-*d*) δ 8.95 (s, 8H), 8.15 (d, *J* = 7.6 Hz, 4H), 8.03 (s, 4H), 7.83 (t, *J* = 7.9 Hz, 4H), 7.62 (d, *J* = 8.5 Hz, 4H), 2.87–2.50 (m, 4H), 2.39–2.20 (m, 4H), 2.03 (td, *J* = 12.1, 10.9, 4.4 Hz, 4H), 1.91–1.74 (m, 4H), 1.21 (s, 12H), 1.18 (s, 12H), 1.16 (s, 12H), −2.86 (s, 2H). ^{13}C NMR (75 MHz, Methylene Chloride-d_2) δ 177.7, 166.5, 148.7, 143.4, 132.7, 128.0, 127.6, 123.0, 119.0, 91.0, 30.9, 29.0, 16.7, 9.5. HR-MS (CSI+): calculated for $[MNa]^+$ ($C_{84}H_{78}N_4O_{16}$): 1421.5310, found: 1421.5351

Zinc porphyrin 4. Porphyrin i4 (100.6 mg, 0.075 mmol) and $Zn(OAc)_2 \cdot 2H_2O$ (327.7 mg, 1.5 mmol) were dissolved in a mixture of DCM (25 ml) and Acetone (10 ml) and stirred for 1.5 h at RT. After this, the solvent was evaporated, the residue was dissolved in EtOAc (50 ml) and washed with H_2O (3×50 ml), dried with $MgSO_4$ and filtered. The product was obtained by evaporation of the solvent, yielding the product as a purple solid (76.3 mg) in 73% yield. ^{1}H NMR (300 MHz, Methylene Chloride-d_2) δ 9.09 (s, 8H), 8.23 (d, *J* = 7.5 Hz, 4H), 8.09 (s, 4H), 7.89 (td, *J* = 7.9, 1.6 Hz, 4H), 7.72–7.56 (m, 4H), 3.03–2.42 (m, 4H), 2.37–2.16 (m, 4H), 2.14–1.95 (m, 4H), 1.76 (dt, *J* = 13.2, 3.4 Hz, 4H), 1.22 (br s, 12H), 1.14 (br m, 12H), 1.12 (br s, 12H). ^{13}C NMR (126 MHz, Chloroform-*d*) δ 177.7, 166.4, 150.1, 148.6, 144.4, 132.6, 127.7, 127.5, 127.5, 120.6, 119.68, 91.0, 30.8, 29.0, 20.6, 16.7, 13.9, 9.4. HR-MS (CSI+): calculated for $[MNa]^+$ ($C_{84}H_{76}N_4O_{16}Zn$): 1483.4445, found: 1483.4431.

Porphyrin **i5**. Under N_2 atmosphere, 5,10,15,20-tetrakis(3-hydroxyphenyl)porphyrin (332.0 mg, 0.49 mmol), (R)-2-methyl butyric acid (432 µl, 2.7 mmol), DMAP (32.9 mg, 0.27 mmol) and DCC (604.7 mg, 2.9 mmol) were added to a Schlenk flask and dissolved in dry THF (20 ml) and stirred at RT for 48 h. After evaporation of the solvent the mixture was purified using column chromatography (SiO_2, Hexane:DCM = 30:70→0:100) yielding the product as a purple solid (294 mg) in 59% yield. ^{1}H NMR (300 MHz, Methylene Chloride-d_2) δ 8.99 (s, 8H), 8.14 (d, *J* = 7.6 Hz, 4H), 7.99 (s, 4H), 7.83 (t, *J* = 7.9 Hz, 5H), 7.58 (ddd, *J* = 8.3, 2.4, 1.1 Hz, 4H), 2.89–2.57 (m, 4H), 1.91 (dt, *J* = 13.6, 7.3 Hz, 4H), 1.70 (dt, *J* = 13.7, 6.9 Hz, 4H), 1.36 (d, *J* = 6.9 Hz, 12H), 1.06 (t, *J* = 7.4 Hz, 12H), −2.87 (s, 2H). ^{13}C NMR (75 MHz, Methylene Chloride-d_2) δ 175.3, 149.6, 143.1, 132.0, 128.0, 127.6, 121.1, 119.1, 41.2, 26.8, 16.4, 11.4. HR-MS (CSI+): calculated for $[MH]^+$ ($C_{64}H_{62}N_4O_8$): 1015.4646, found 1015.4659

Zinc porphyrin **5**. Porphyrin **i5** (100.2 mg, 0.10 mmol) and $Zn(OAc)_2 \cdot 2H_2O$ were dissolved in a mixture of DCM (25 ml) and Acetone (10 ml) and stirred for 1.5 h at RT. After this, the solvent was evaporated, the residue was dissolved in EtOAc (50 ml) and washed with H_2O (3×50 ml), dried with $MgSO_4$ and filtered. The product was obtained by evaporation of the solvent, yielding the product as a purple solid (89.9 mg) in 89% yield. ^{1}H NMR (300 MHz, Methylene Chloride-d_2) δ 9.07 (br s, 8H), 8.14 (d, *J* = 7.6 Hz, 4H), 7.99 (s, 4H), 7.82 (t, *J* = 7.9 Hz, 4H), 7.56 (d, *J* = 8.1 Hz, 4H), 2.75 (q, *J* = 6.9 Hz, 4H), 1.91 (dt, *J* = 14.3, 7.2 Hz, 4H), 1.70 (dt, *J* = 14.3, 7.2 Hz, 4H), 1.35 (d, *J* = 6.9 Hz, 12H), 1.06 (t, *J* = 7.4 Hz, 12H). ^{13}C NMR (126 MHz, $CDCl_3$) δ 175.3, 149.5, 143.9, 132.1, 131.9, 127.9, 127.4, 120.8, 120.0, 41.2, 26.8, 16.4, 14.0, 11.4. HR-MS (CSI+): calculated for $[MNa]^+$ ($C_{64}H_{60}N_4O_8Zn$): 1099.3600, found: 1099.3670

Acknowledgements

We thank the European Research Council (ERC Adv. Grant 339786-NAT_CAT to Reek) for financial support. We would like to thank dr. J. Heinen for DFT calculations and P.R. Linnenbank for performing control experiments.

Conflict of Interest

The authors declare no conflict of interest.

Keywords: catalyst encapsulation · hydroformylation · supramolecular chemistry · asymmetric catalysis · bio-inspired catalysis

[1] P. W. N. M. van Leeuwen, *Focus Catal.* **2005**, *2005*, 8.

[2] M. Raynal, P. Ballester, A. Vidal-Ferran, P. W. N. M. Van Leeuwen, *Chem. Soc. Rev.* **2014**, *43*, 1660–1733.
[3] M. Raynal, P. Ballester, A. Vidal-Ferran, P. W. N. M. van Leeuwen, *Chem. Soc. Rev.* **2014**, *43*, 1734–1787.
[4] S. H. A. M. Leenders, R. Gramage-Doria, B. de Bruin, J. N. H. Reek, *Chem. Soc. Rev.* **2015**, *44*, 433–448.
[5] C. J. Brown, F. D. Toste, R. G. Bergman, K. N. Raymond, *Chem. Rev.* **2015**, *115*, 3012–3035.
[6] W. X. Gao, H. N. Zhang, G. X. Jin, *Coord. Chem. Rev.* **2019**, *386*, 69–84.
[7] C. Tan, D. Chu, X. Tang, Y. Liu, W. Xuan, Y. Cui, *Chem. Eur. J.* **2019**, *25*, 662–672.
[8] C. M. Hong, R. G. Bergman, K. N. Raymond, F. D. Toste, *Acc. Chem. Res.* **2018**, *51*, 2447–2455.
[9] V. Blanco, D. A. Leigh, V. Marcos, *Chem. Soc. Rev.* **2015**, *44*, 5341–5370.
[10] M. J. Wiester, P. A. Ulmann, C. A. Mirkin, *Angew. Chem. Int. Ed.* **2011**, *50*, 114–137; *Angew. Chem.* **2011**, *123*, 118–142.
[11] U. Lüning, *Angew. Chem. Int. Ed.* **2012**, *51*, 8163–8165; *Angew. Chem.* **2012**, *124*, 8285–8287.
[12] T. Imahori, S. Kurihara, *Chem. Lett.* **2014**, *43*, 1524–1531.
[13] A. J. McConnell, C. S. Wood, P. P. Neelakandan, J. R. Nitschke, *Chem. Rev.* **2015**, *115*, 7729–7793.
[14] M. Vaquero, L. Rovira, A. Vidal-Ferran, *Chem. Commun.* **2016**, *52*, 11038–11051.
[15] M. Vlatković, B. S. L. Collins, B. L. Feringa, *Chem. Eur. J.* **2016**, *22*, 17080–17111.
[16] J. A. A. W. Elemans, E. J. A. Bijsterveld, A. E. Rowan, R. J. M. Nolte, *Eur. J. Org. Chem.* **2007**, 751–757.
[17] L. J. Jongkind, J. A. A. W. Elemans, J. N. H. Reek, *Angew. Chem. Int. Ed.* **2019**, *58*, 2696–2699.
[18] A. C. H. Jans, A. Gómez-Suárez, S. P. Nolan, J. N. H. Reek, *Chem. Eur. J.* **2016**, *22*, 14836–14839.
[19] M. Yoshizawa, M. Tamura, M. Fujita, *Science* **2006**, *312*, 251–255.
[20] J. Kang, J. Rebek, *Nature* **1996**, *382*, 239–241.
[21] Q. Zhang, L. Catti, K. Tiefenbacher, *Acc. Chem. Res.* **2018**, *51*, 2107–2114.
[22] S. H. A. M. Leenders, R. Gramage-Doria, B. de Bruin, J. N. H. Reek, *Chem. Soc. Rev.* **2015**, *44*, 433–448.
[23] Q. Q. Wang, S. Gonell, S. H. A. M. Leenders, M. Dürr, I. Ivanovic-Burmazovic, J. N. H. Reek, *Nat. Chem.* **2016**, *8*, 225–230.
[24] R. Gramage-Doria, J. Hessels, S. H. A. M. Leenders, O. Tröppner, M. Dürr, I. Ivanović-Burmazović, J. N. H. Reek, *Angew. Chem. Int. Ed.* **2014**, *53*, 13380–13384; *Angew. Chem.* **2014**, *126*, 13598–13602.
[25] L. J. Jongkind, X. Caumes, A. P. T. Hartendorp, J. N. H. Reek, *Acc. Chem. Res.* **2018**, *51*, 2115–2128.
[26] V. F. Slagt, J. N. H. Reek, P. C. J. Kamer, P. W. N. M. Van Leeuwen, *Angew. Chem. Int. Ed.* **2001**, *40*, 4271–4274; *Angew. Chem.* **2001**, *113*, 4401–4404.
[27] V. F. Slagt, P. C. J. Kamer, P. W. N. M. Van Leeuwen, J. N. H. Reek, *J. Am. Chem. Soc.* **2004**, *126*, 1526–1536.
[28] V. Bocokić, A. Kalkan, M. Lutz, A. L. Spek, D. T. Gryko, J. N. H. Reek, *Nat. Commun.* **2013**, *4*, 1–9.
[29] T. Besset, D. W. Norman, J. N. H. Reek, *Adv. Synth. Catal.* **2013**, *355*, 348–352.
[30] V. Bocokić, Supramolecular Encapsulation of a Rhodium Hydroformylation Catalyst: A Mechanistic Study, **2011**.
[31] R. Bellini, J. N. H. Reek, *Eur. J. Inorg. Chem.* **2012**, *2012*, 4684–4693.
[32] R. Bellini, J. N. H. Reek, *Chem. Eur. J.* **2012**, *18*, 13510–13519.
[33] R. Bellini, S. H. Chikkali, G. Berthon-Gelloz, J. N. H. Reek, *Angew. Chem. Int. Ed.* **2011**, *50*, 7342–7345; *Angew. Chem.* **2011**, *123*, 7480–7483.
[34] D. Ringe, G. A. Petsko, *Science* **2008**, *320*, 1428–1429.
[35] I. Jacobs, A. C. T. van Duin, A. W. Kleij, M. Kuil, D. M. Tooke, A. L. Spek, J. N. H. Reek, *Catal. Sci. Technol.* **2013**, *3*, 1955.
[36] I. Jacobs, Insights In Rhodium-Catalyzed Hydroformylation In Supramolecular Cages A Combined Experimental and Theoretical Approach, **2015**.
[37] Y. Chen, K. B. Fields, X. P. Zhang, *J. Am. Chem. Soc.* **2004**, *126*, 14718–14719.
[38] T. Jongsma, G. Challa, P. W. N. M. van Leeuwen, *J. Organomet. Chem.* **1991**, *421*, 121–128.
[39] X. Wang, S. S. Nurttila, W. I. Dzik, R. Becker, J. Rodgers, J. N. H. Reek, *Chem. Eur. J.* **2017**, *23*, 14769–14777.
[40] T. Gadzikwa, R. Bellini, H. L. Dekker, J. N. H. Reek, *J. Am. Chem. Soc.* **2012**, *134*, 2860–2863.
[41] A. M. Kluwer, I. Ahmad, J. N. H. Reek, *Tetrahedron Lett.* **2007**, DOI 10.1016/j.tetlet.2007.02.127.
[42] P. C. J. Kamer, A. van Rooy, G. C. Schoemaker, P. W. N. M. van Leeuwen, *Coord. Chem. Rev.* **2004**, *248*, 2409–2424.

Manuscript received: December 17, 2019
Revised manuscript received: January 17, 2020
Accepted manuscript online: February 5, 2020
Version of record online: February 21, 2020